Copy
RM E57I12




NACA RM E57I12



# RESEARCH MEMORANDUM

## EXPERIMENTAL INVESTIGATION OF DISTORTION REMOVAL CHARACTERISTICS OF SEVERAL FREE-WHEELING FANS

By Harold H. Valentine and William T. Beale

Lewis Flight Propulsion Laboratory
Cleveland, Ohio



CLASSIFIED DOCUMENT



NATIONAL ADVISORY COMMITTEE
FOR AERONAUTICS

WASHINGTON

January 7, 1958

NATIONAL ADVISORY COMMITTEE FOR AERONAUTICS

RESEARCH MEMORANDUM

# EXPERIMENTAL INVESTIGATION OF DISTORTION REMOVAL CHARACTERISTICS OF SEVERAL FREE-WHEELING FANS

By Harold H. Valentine and William T. Beale



## SUMMARY

In an investigation of the distortion removal performance and associated total-pressure-loss characteristics of several freely rotating fans, three single-stage and two double-stage freely rotating fans were run over a range of radial and circumferential distortions of from 0 to 20 percent at inlet annulus Mach numbers from 0.30 to about 0.60. All the fans tested were more effective in removing radial distortions than circumferential distortions. High-solidity fans more effectively removed distortion than low-solidity fans, but the high-solidity fans suffered more than proportionally greater total-pressure losses. Increasing the blade stagger angle from 45° to 60° increased the distortion removal performance.

The high-solidity fans choked at Mach numbers of 0.50 to 0.60, and it looks doubtful if any but the single-stage, low-solidity fan would remain unchoked at Mach 0.70.

It appears that freely rotating fans can remove about one-half of the radial distortion and about one-third of the circumferential distortion at the expense of a total-pressure loss of about $1\frac{1}{2}$ to $2\frac{1}{2}$ percent.

## INTRODUCTION

Inlet air distortions (velocity and pressure variations) at the face of aircraft engine compressors are influenced by the inlet configuration and may be caused by bends or obstructions in the duct, various flight maneuvers, and/or by shock patterns at supersonic inlets. These inlet distortions may necessitate engine derating in order to avoid turbine burnout due to local hot spots and also may reduce altitude limits and the acceleration margin of the engine by inducing surge and stall phenomena. Several approaches may be used to solve this problem: the engine can be redesigned to reduce distortion sensitivity, the inlet duct can be redesigned, or a corrective device can be installed to reduce the

degree of distortion to an acceptable level. (Several types of corrective devices under consideration are screens, vortex generators, mixing sections, lip bleed, and freely rotating fans.) Inasmuch as all approaches penalize the aircraft in one way or another, a comparative analysis of engine redesign, duct redesign, and corrective devices is necessary for each case where this problem exists.

Some of the earliest work with freely rotating fans to remove air distortion is reported in references 1 and 2. These investigations were limited to flow at low Mach numbers. Reference 3 is a theoretical analysis of single-stage, freely rotating fans removing radial distortion. In order to determine the distortion removing characteristics of freely rotating fans at annulus Mach numbers of about 0.50, the investigation reported herein was undertaken.

The distortion removal capabilities and associated total-pressure losses of three single-stage and two double-stage fans were obtained for a range of radial and circumferential distortions of from 0 to 20 percent at fan inlet annulus Mach numbers from 0.30 to about 0.60. All the fans tested had hub-tip radius ratios of 0.53, and design speeds ranged from 7400 to 12,800 rpm at an inlet annulus Mach number of 0.50. Four of the fans tested had identical blade stagger angles ($45^\circ$ at the tip) and differed by number of stages and/or solidity. The fifth fan tested had larger blade stagger angles ($60^\circ$ at the tip).

The fans were tested in a connected pipe test rig using laboratory service air at ambient temperature. The annulus Mach number was varied by varying the exhaust pressure.

The distortion removal performance of each fan is presented for inlet annulus Mach numbers of 0.40, 0.50, and 0.55. Fan comparisons are made on the basis of distortion removal.

## SYMBOLS

D distortion magnitude (measured at station 2), percent

E ratio of distortion removal to initial distortion, $(D_n - D_f)/D_n$, percent

P total pressure, lb/sq ft

r radius, in.

U wheel speed of fan at a given radius r, ft/sec

V average axial velocity of flow through annulus, ft/sec

$\beta$ fan-blade stagger angle, deg

Subscripts

av area-weighted average of all 40 total-pressure readings at a given station

f with fan installed in annulus

l individual reading

max highest reading single probe

max av for radial distortions, the highest of the five averages obtained by averaging the eight total-pressure readings at each radius across the annulus; for circumferential distortions, the highest of the eight averages obtained by averaging the five total-pressure readings at each 45° position around the annulus

min lowest reading single probe

min av for radial distortions, the lowest of the five averages explained previously for radial distortions; for circumferential distortions, the lowest of the eight averages explained previously for circumferential distortions

n without fan installed in annulus

1 measuring station upstream of fan

2 measuring station downstream of fan

## APPARATUS

All five fans tested had a hub-tip radius ratio of 0.53 and a tip diameter of 17.74 inches. Circular arc blade profiles with zero camber as shown in figure 1 were used on all fans. The blades were designed to have zero angle of attack with undistorted flow. The following table gives the basic geometry of each fan. Solidity is defined as the blade chord-to-pitch ratio. The blade angle (stagger angle) is defined by the relation $\tan \beta = U/V$ where U is the wheel speed at some radius r and V is the axial velocity of the flow. The blade twist is the difference between the stagger angles at the tip and the root of the blade.

| | Fan | | | | |
|---|---|---|---|---|---|
| | 1 | 2 | 3 | 4 | 5 |
| Number of stages | 1 | 1 | 1 | 2 | 2 |
| Number of blades | 16 | 32 | 15 | 15 Fore<br>16 Aft | 30 Fore<br>32 Aft |
| Maximum blade thickness, in. | 0.19 | 0.19 | 0.13 | 0.19 | 0.19 |
| Tip solidity | 0.793 | 1.586 | 0.865 | 0.743 Fore<br>.793 Aft | 1.486 Fore<br>1.586 Aft |
| Blade tip angle, deg | 45 | 45 | 60 | 45 | 45 |
| Twist along blade | 17°15' | 17°15' | 17°30' | 17°15' | 17°15' |

Photographs of fans 2, 3, and 4 are presented in figures 2, 3, and 4, respectively. Fan 1 was made by removing every other blade on fan 2, and fan 5 was made by doubling the number of blades on each stage of fan 4. Figure 5 presents the installation showing the location of the fans, the distortion-producing screens, and the measuring stations. During testing the bullet nose was located as illustrated in figure 5 and not as shown in figures 2, 3, and 4.

The various configurations of the distortion-producing screens used are illustrated in figure 6. The crosshatched areas represent the screens. Screen blockages of 32, 49, and 72 percent were used to produce the radial distortions, but only 32- and 49-percent blockages were used in producing circumferential distortions. The screens producing radial distortion covered half the annulus width.

Total- and static-pressure measurements were taken at stations 1 and 2 to determine Mach number, total-pressure losses, and distortion levels. As illustrated in figure 7, eight total-pressure rakes of five tubes each were located at each station. Four wall static tubes were located at station 1 and six at station 2 at the positions shown in figure 7.

## PROCEDURE

Total-pressure-loss data for undistorted flow were taken over the Mach number range of 0.30 to 0.60 with each fan installed and with no fan

installed. These data were all plotted against the Mach number measured at station 1. The total-pressure-loss curve for each fan was then determined by the difference between the curves for the annulus with and without the fan.

In a similar manner, the distortion removal performance of each fan was obtained by data that would determine the distortion level at station 2, first without a fan in the annulus and then with a fan in the annulus, for a given value of distortion at station 1. The distortion removal by the fan was then the difference between the distortions measured at station 2 with and without the fan. In addition to pressure loss and distortion, the fan speed was also measured at every datum point.

## METHOD OF DATA PRESENTATION

Distortion magnitude has usually been defined in the literature as $(P_{max} - P_{min})/P_{av}$ (refs. 4, 5, and 6). Distortions based on this definition shall herein be referred to as point distortions. The use of this definition in the present investigation resulted in scatter and inconsistencies in the data. In order to reduce the scatter and provide a firmer basis for fan comparisons, distortion magnitude was redefined on an average basis. Figure 7 is useful in describing the averaging technique used. (Eight circumferential positions were instrumented with total-pressure tubes at each of five radial positions.) For radial distortions, the eight total pressures at each radius were arithmetically averaged. The highest of the five resulting averages was termed $P_{max\ av}$, and the lowest average was termed $P_{min\ av}$. The distortion magnitude was then $(P_{max\ av} - P_{min\ av})/P_{av}$ where $P_{av}$ was the average of all the readings across the annulus.

The magnitudes of the circumferential distortions were obtained by averaging the five readings at each circumferential position around the annulus. The highest of the resulting eight averages was termed $P_{max\ av}$, and the lowest was termed $P_{min\ av}$. Again, the distortion magnitude was expressed as $(P_{max\ av} - P_{min\ av})/P_{av}$. All the distortions referred to in this report are based on this average distortion method unless otherwise indicated.

Typical distortion profiles illustrating the difference between point and average distortion are presented in figure 8. Changes in the flow profile resulting from the action of the fan are also shown in these figures.

The performance of each fan is presented in plots that were determined by cross-plotting the basic fan data at several constant values of Mach number. Thus, no actual data points are considered in the following section, RESULTS AND DISCUSSION. Typical distortion basic data plots for one of the fans (the low-solidity, high-blade-angle fan) are shown in figure 9. In order to obtain a true evaluation of the fan performance, the distortion level at station 1 should be the same with or without a fan. Figure 9 shows that this condition was maintained closely over the Mach number range covered.

The parameters used to describe the performance of the fans are fan distortion effectiveness and fan total-pressure loss, wherein the fan effectiveness E is defined as the distortion removal expressed in percent of the initial distortion $E = (D_n - D_f)/D_n$, and the fan total-pressure loss is defined as the difference between the area-weighted total-pressure loss of the annulus with the fan and the annulus alone as measured between stations 1 and 2 with undistorted flow.

Inasmuch as both magnitude and distribution (or extent) are necessary to specify a distortion adequately, and inasmuch as only magnitudes are given in this report, some typical total-pressure contours are presented in figure 10 to illustrate the extent of the distortions used.

## RESULTS AND DISCUSSION

### Individual Fan Performance

The performance data for each of the five fans tested are presented in figure 11. The fan effectiveness E is plotted against percent input distortion. Separate curves are presented for each type of distortion used, and data are presented for three values of annulus Mach number (measured at station 1), 0.40, 0.50, and 0.55.

For each fan tested, the effects on fan performance of the input distortion level, the distortion type, and the Mach number are discussed. The fans are considered in the order of decreasing performance. Inasmuch as the distortion level generally increases with Mach number, three values of input distortion, 6, 12, and 18 percent, representing conditions at Mach numbers 0.40, 0.50, and 0.55, respectively, have been chosen arbitrarily for discussing the effect of Mach number on fan performance.

Two-stage, high-solidity fan. - The performance data for the two-stage, high-solidity (30- and 32-blade) fan are presented in figure 11(a). Since this fan choked at an annulus Mach number of 0.525, no data are presented at Mach 0.55. This fan was most effective in removing inner radial distortion and least effective in removing circumferential distortion. In general, for a constant annulus Mach number there was a marked

increase in fan effectiveness with all three types of distortion as the input distortion level increased. Between Mach numbers 0.40 (6-percent distortion) and 0.50 (12-percent distortion) the effectiveness increased from 39 to 46 percent with outer radial distortion and from 52 to 54 percent with inner radial distortion. With circumferential distortion, however, the effectiveness decreased from 52 to 42 percent between Mach 0.40 and 0.50.

Single-stage, low-solidity, high-blade-angle fan. - The performance data for the single-stage, low-solidity, high-blade-angle ($60^{\circ}$ at tip) fan are presented in figure 11(b). In general, this fan was much more effective in removing radial distortions than circumferential distortions, and at the lower distortion levels it was more effective in removing inner radial distortions than outer radial distortions. At each annulus Mach number the fan effectiveness with inner radial distortion was initially very high, with a steady decrease as the input distortion level increased. It is not clear why this fan was so effective at the lower distortion levels with inner radial distortion. (A similar characteristic was obtained with the single-stage, high-solidity (32-blade) fan (fig. 11(d)).

At the distortion levels picked for discussion (6, 12, and 18 percent), the effectiveness decreased with inner radial distortion from 70 percent at Mach 0.40 (6-percent distortion) to about 60 percent at Mach 0.55 (18-percent distortion) (fig. 11(b)). Similarly, with circumferential distortion, the effectiveness decreased from 18 percent at Mach 0.40 to 11 percent at Mach 0.55. In contrast, as Mach number and distortion level increased, the effectiveness increased with outer radial distortion from 42 percent at Mach 0.40 to 52 percent at Mach 0.55.

Two-stage, low-solidity fan. - The distortion removal performance of the two-stage, low-solidity (15- and 16-blade) fan is presented in figure 11(c). Generally, this fan was most effective when removing inner radial distortion and least effective when removing circumferential distortion. There was a general trend with all three types of distortion toward an increase in effectiveness as the input distortion level increased at each Mach number. With both inner radial and circumferential distortions, fan effectiveness remained constant at 50 and 36 percent, respectively, as Mach number and distortion level increased. With outer radial distortion, the effectiveness increased from 32 percent at Mach 0.40 (6-percent distortion) to 46 percent at Mach 0.55 (18-percent distortion).

Single-stage, high-solidity fan. - The performance data for the single-stage high-solidity (32-blade) fan are presented in figure 11(d). As with the single-stage, high-blade-angle fan, this fan was much more effective in removing inner radial distortions than in removing the other two types. For a constant Mach number, the fan effectiveness increased as the input level increased with both outer radial and circumferential

distortions, but with inner radial distortion an increase in the distortion input level resulted in a decrease in fan effectiveness. Between Mach 0.40 and 0.55, the effectiveness increased from 19 to 24 percent and from 22 to 35 percent for circumferential and outer radial distortions, respectively. With inner radial distortion, the effectiveness remained about 39 percent as Mach number increased.

Single-stage, low-solidity fan. - The distortion removal performance of the single-stage, low-solidity (16-blade) fan is presented in figure 11(e). This fan also was much more effective in removing inner radial distortions than outer radial distortions. Insufficient data were taken with circumferential distortions to cross-plot the performance, but the limited data taken indicated very low performance. In general, for a constant Mach number the effectiveness increased 1.5 to 2.0 percentage points for every percentage point increase in the distortion input level. Between Mach 0.40 (6-percent distortion) and Mach 0.55 (18-percent distortion) the fan effectiveness increased from 12 to 25 percent with outer radial distortion and from 28 to 40 percent with inner radial distortion.

## Comparison of Fan Distortion Removal Characteristics

The distortion removal performance of each fan at an annulus Mach number of 0.50 has been plotted in figure 12 in order to compare the various fans. The two-stage, high-solidity fan appears to have been the most effective fan tested from the standpoint of distortion removal. The single-stage, high-blade-angle fan was just as effective with radial distortions (more effective with inner radial distortion), but it was very poor in removing circumferential distortions. The remaining fans in the order of decreasing performance are the two-stage, low-solidity fan, the single-stage, high-solidity fan, and the single-stage, low-solidity fan.

Effect of distortion level. - Figure 12(a) shows that, for all the fans tested, the fan effectiveness increased substantially as the outer radial distortion level increased. With inner radial distortion (fig. 12(b)), the effectiveness increased with distortion level for the two-stage fans and the single-stage, low-solidity fan, but the other two single-stage fans exhibited high initial values of effectiveness with a steady decline as the distortion level increased. The reason for this phenomenon is not understood.

All the fans show a moderate increase in effectiveness with distortion level for circumferential distortions (fig. 12(c)).

Effect of number of stages. - In general, the effectiveness of the two-stage fans was over 50 percent better than that of the corresponding

single-stage fans. For example, with outer radial distortion (fig. 12(a)) the two-stage high-solidity fan had an effectiveness of 54 percent at an input distortion level of 16 percent, while the effectiveness of the single-stage, high-solidity fan was only 27 percent at the same input distortion level. In addition to a better redistribution of the flow, the second stage tends to remove the swirl introduced by the first stage.

Effect of solidity. - Increasing the solidity increased the fan effectiveness of both the single- and double-stage fans for all three types of distortion. Increasing the solidity provides more guidance for the flow, and, hence, a better redistribution of energy occurs than with a lower solidity fan.

Effect of blade angle. - With radial distortion, increasing the blade angle substantially increased the fan effectiveness. The single-stage fan with 60° blade tip angles was over 60 percent more effective than the single-stage, low-solidity fan with 45° blade tip angles. This is as expected since energy transfer is a function of the wheel speed, and the wheel speed is proportional to the tangent of the blade angle.

Effect of distortion extent. - Because a freely rotating fan removes distortion by transferring energy from the high-velocity region of the stream to the low-velocity region of the stream, the extent of the input distortion obviously affects the fan performance. As the percentage of the annulus area exposed to high-velocity air increases, the fan effectiveness should increase. As previously stated, during this investigation the distortion-producing screens covered half the annulus width, which resulted in rather extensive distortions. Undoubtedly, higher fan performance would be obtained with less extensive distortions, and, conversely, poorer performance would be obtained with more extensive distortions.

Effect of distortion calculation method. - As explained in the section METHOD OF DATA PRESENTATION, the distortion magnitude referred to in this report was calculated through the use of a total-pressure averaging technique. In the reference literature, distortion magnitude has usually been calculated from two single pressure readings, the maximum and the minimum. In order to get a comparison of the two methods, the data of figure 12 were replotted in figure 13 on the single pressure or point distortion basis. Comparing figure 13 with figure 12 results in the following generalizations:

(1) Calculating the input distortion level on the point basis resulted in magnitudes about 10 to 20 percent higher than those calculated on the average basis.

(2) The fan effectiveness was generally slightly lower when calculated from point distortion values than when calculated from average distortion values.

(3) In general, the relative order of the fans in terms of performance was the same with either method.

### Fan Total-Pressure Loss and Operating Speed Characteristics

The undistorted total-pressure losses and operating speeds of each of the fans tested are plotted in figure 14 against the inlet annulus Mach number (at station 1). Undistorted flow data were used in this plot because they were considered more reliable over the entire range of conditions covered. Spot checks between these data and distorted flow data wherein the pressure loss was computed from area-weighted total-pressure measurements indicated that there was good agreement and that within the accuracy of the data there was no effect of distortion on the pressure drop. The accuracy of the pressure drop data is estimated to be within $\pm 1/2$ of one percentage point. (For example, from fig. 14 the total-pressure loss for the single-stage, high-blade-angle fan at Mach 0.50 is 3.3 percent, whereas the actual loss may be anywhere between 2.7 and 3.8 percent.)

As would be expected, the low-solidity fans with 45° tip angles (both one- and two-stage) exhibited the least total-pressure loss. In addition, they had little increase in total-pressure loss up to Mach number 0.65. The two-stage, high-solidity fan exhibited the greatest increase in pressure loss with Mach number, and at Mach 0.525 this fan was choked, as evidenced by the rapid increase in pressure loss. The high-blade-angle fan, while having about twice the pressure loss of the other fans at Mach 0.30, experienced a more gradual increase with Mach number than the high-solidity fans.

The speed lines for the two low-solidity fans and the high-blade-angle fan are approximately linear and in general verify the predicted values. The speed lines for the two high-solidity fans show more curvature, since choking begins at a lower annulus Mach number for these fans.

## CONCLUDING REMARKS

Five freely rotating fans were tested for distortion removal performance over a range of radial and circumferential distortions from 0 to 20 percent at inlet annulus Mach numbers from 0.30 to about 0.60. The results may be summarized as follows:

1. The two-stage counterrotating fans were over 50 percent more effective in removing distortion than the single-stage fans having identical blading.

2. Increasing the blade stagger angle increased the distortion removal performance. The single-stage fan with blade tip angles of 60° was over 60 percent more effective in removing distortion than the single-stage, low-solidity fan with 45° blade tip angles.

3. High-solidity fans were more effective in removing distortion than low-solidity fans but suffered more than proportionally greater total-pressure losses.

4. The fans tested were more effective in removing radial distortion than circumferential distortion. This was especially true of the single-stage, low-solidity, high-blade-angle fan.

Two significant conclusions that may be drawn from the above investigation are:

1. High-solidity fans choked at Mach numbers of 0.50 to 0.60. It looks doubtful if any but the low-solidity, single-stage fan would remain unchoked at Mach 0.70.

2. Freely rotating fans can remove about one-half the radial distortion and about one-third the circumferential distortion at the expense of a total-pressure loss of about $1\frac{1}{2}$ to $2\frac{1}{2}$ percent.

Lewis Flight Propulsion Laboratory
National Advisory Committee for Aeronautics
Cleveland, Ohio, October 1, 1957

## REFERENCES

1. Collar, A. R.: The Use of a Freely Rotating Windmill to Improve the Flow in a Wind Tunnel. R. & M. No. 1866, British ARC, Nov. 23, 1938.

2. Johnston, I. H.: The Use of Freely Rotating Blade Rows to Improve Velocity Distribution in an Annulus. Memo. No. M.109, British NGTE, Feb. 1951.

3. English, Robert E., and Yohner, Peggy L.: Theoretical Analysis of One-Stage Windmills for Reducing Flow Distortion. NACA RM E57D05, 1957.

4. Klann, John L.: Experimental Evaluation of Methods for Improving Diffuser-Exit Total-Pressure Profiles for a Side-Inlet Model at Mach Number 1.91. NACA RM E56K05a, 1957.

5. Piercy, Thomas G., and Klann, John L.: Experimental Investigation of Methods of Improving Diffuser-Exit Total-Pressure Profiles for a Side-Inlet Model at Mach Number 3.05. NACA RM E55F24, 1955.

6. Wallner, Lewis E., Conrad, E. William, and Prince, William R.: Effect of Uneven Air-Flow Distribution to the Twin Inlets of an Axial-Flow Turbojet Engine. NACA RM E52K06, 1953.

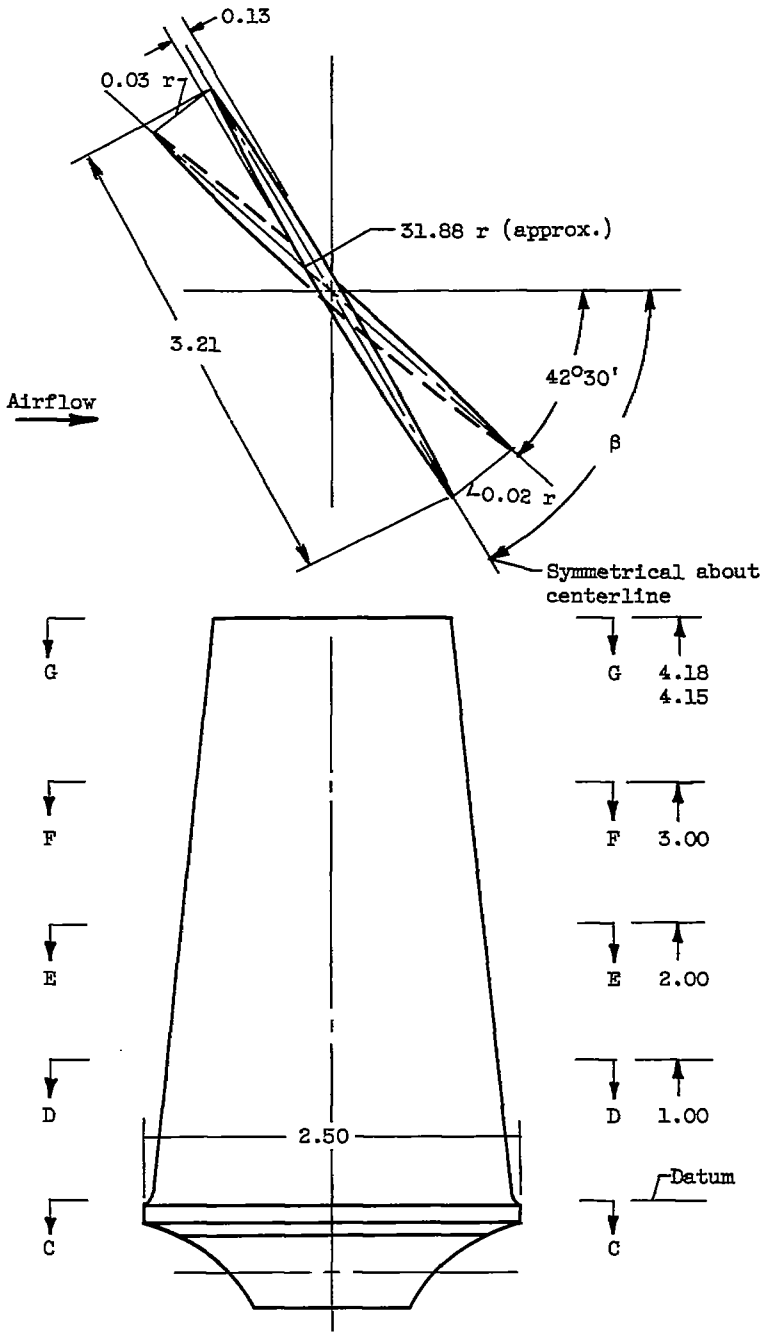


| Angle | C-C | D-D | E-E | F-F | G-G |
|---|---|---|---|---|---|
| β | 42°30' | 48°4' | 52°38' | 56°24' | 60°0' |

(a) 60°-Tip-angle fan.

Figure 1. - Blade design. (All dimensions in inches except where noted.)

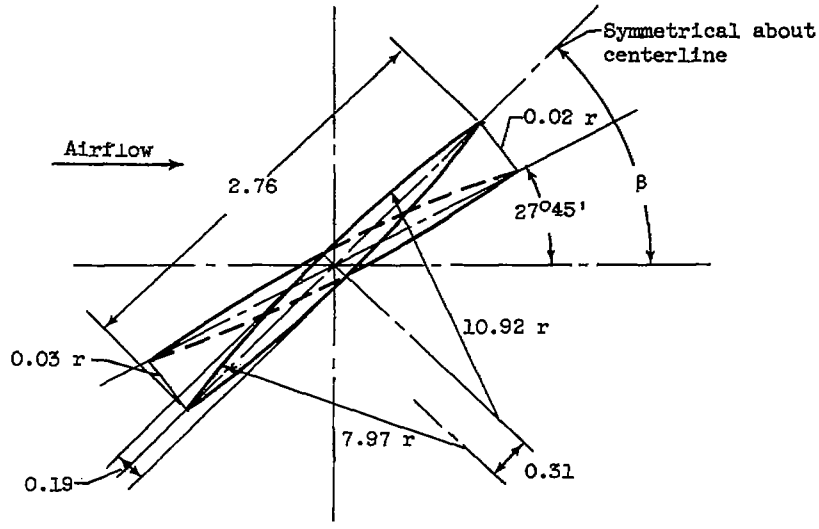


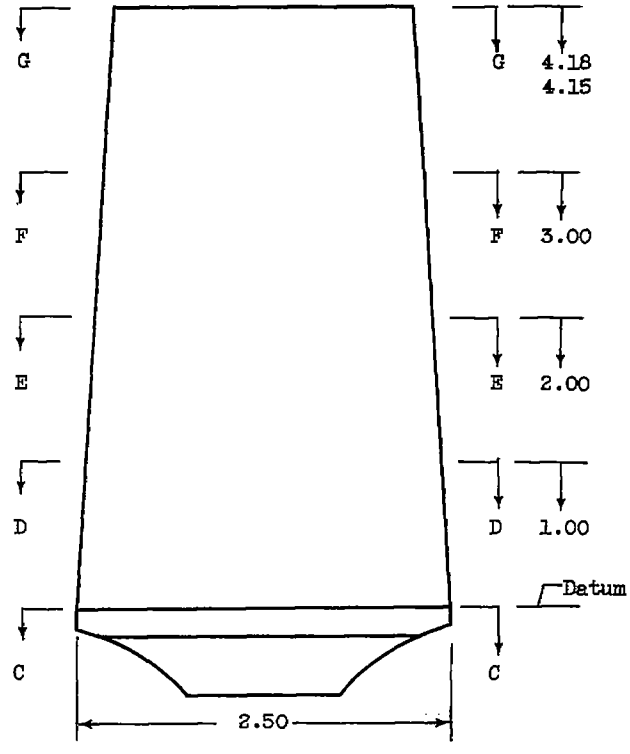


| Angle | C-C | D-D | E-E | F-F | G-G |
|---|---|---|---|---|---|
| β | 27°45' | 32°45' | 36°45' | 40°45' | 45°0' |

(b) 45°-Tip-angle fans.

Figure 1. - Concluded. Blade design. (All dimensions in inches except where noted.)

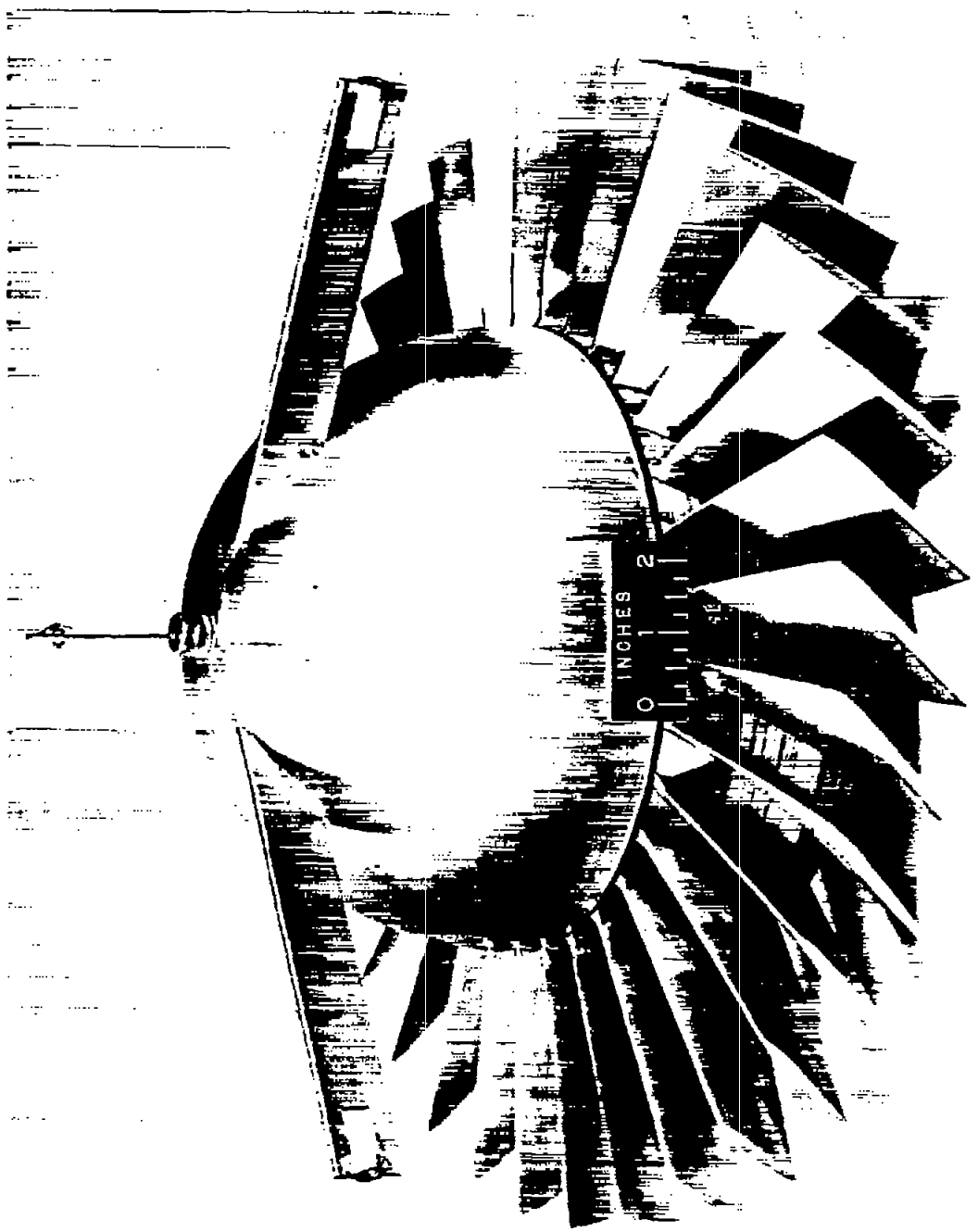


C-39191

Figure 2. - Fan 2 (single stage, high solidity).


Figure 3. - Fan 3 (single stage, low solidity, high blade angle).

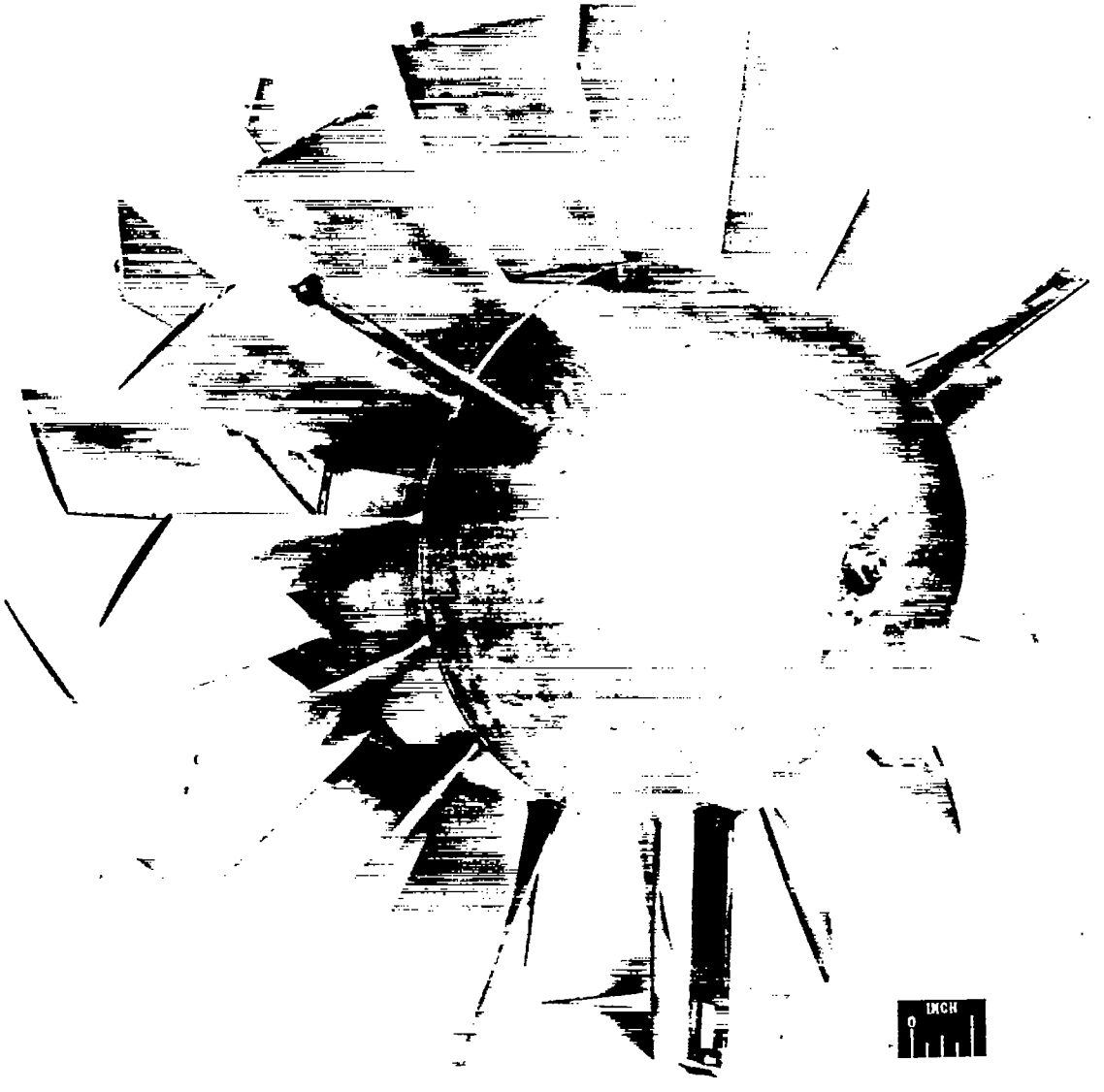


Figure 4. - Fan 4 (two stage, low solidity).

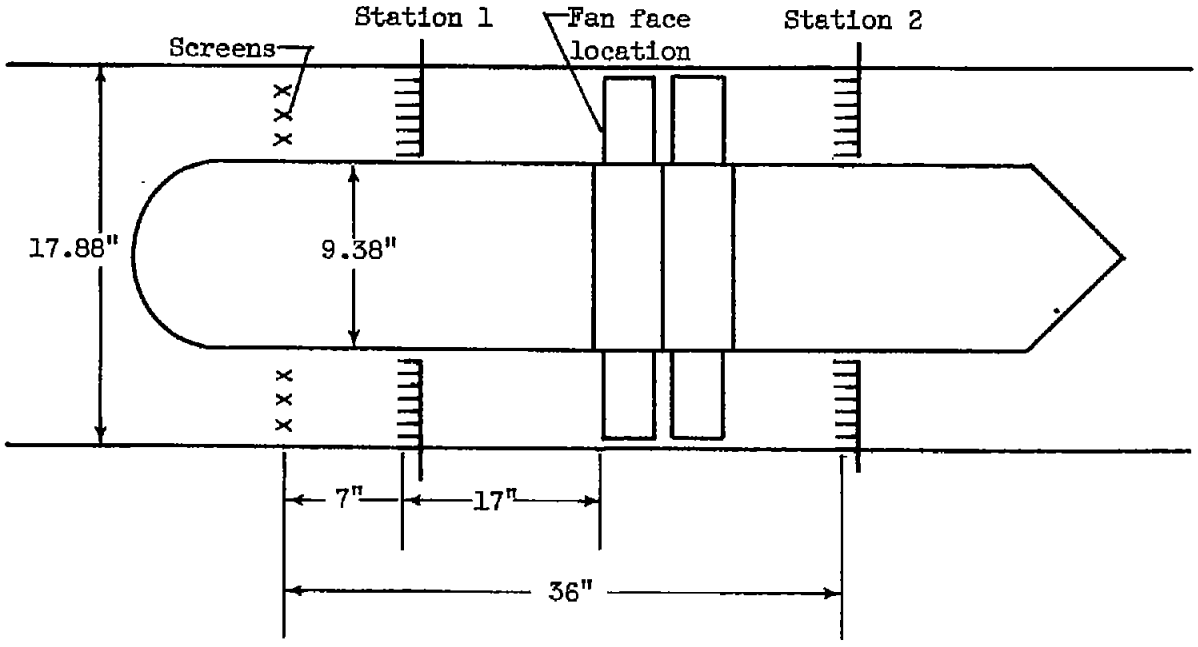


Figure 5. - Schematic diagram of installation showing location of fans, screens, and measuring stations.

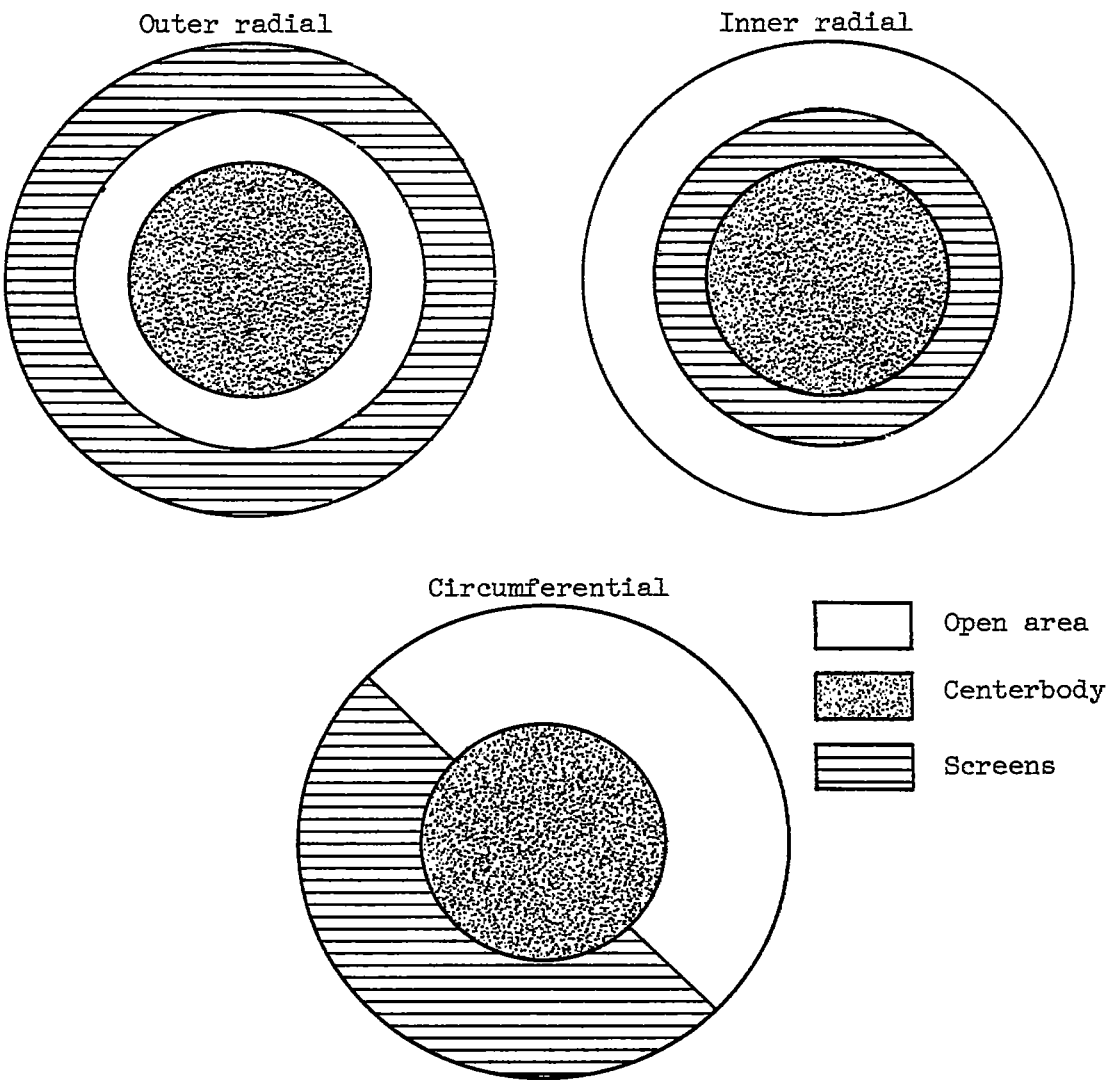


Figure 6. - Screen configurations used to produce distortion.

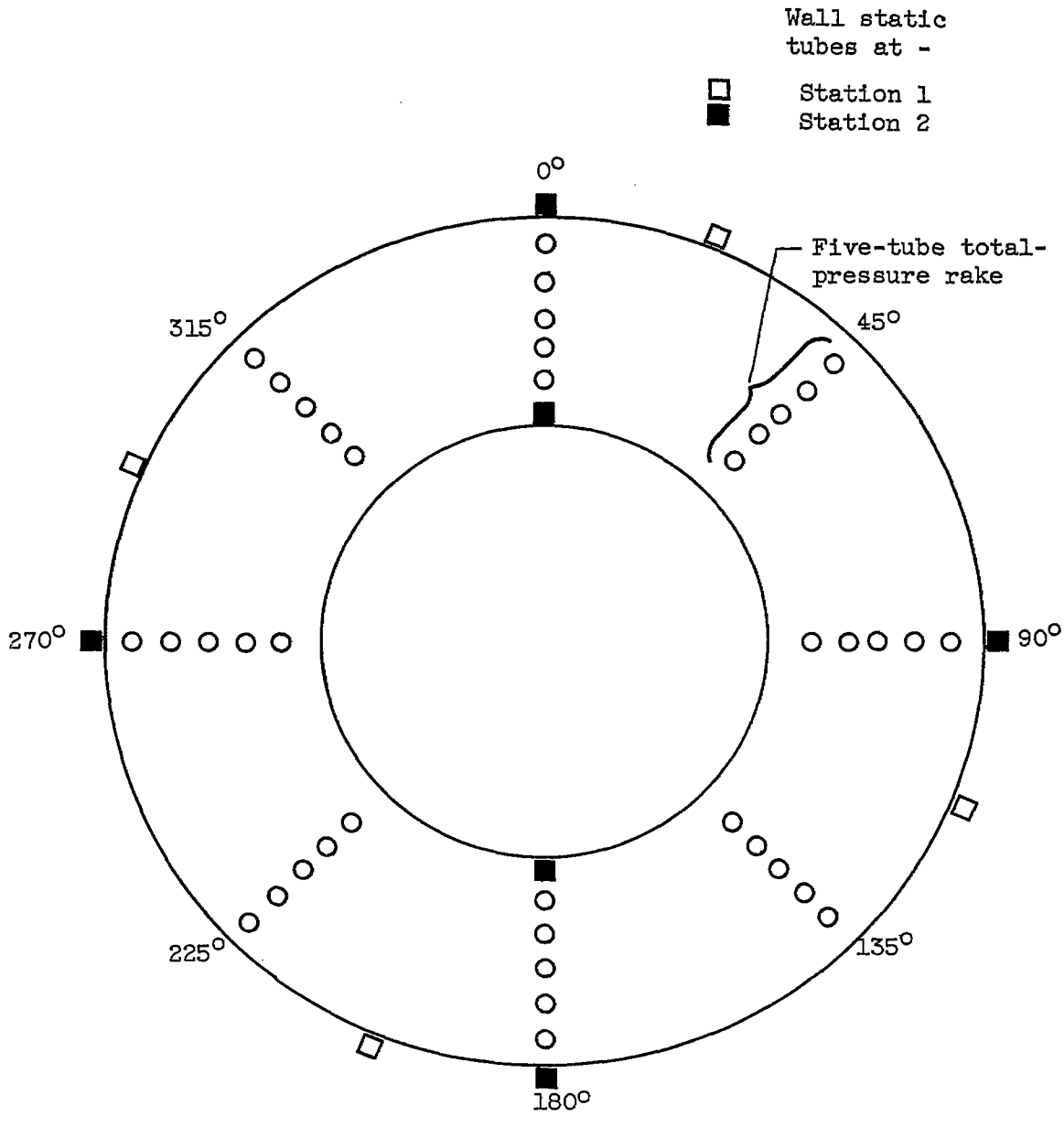


Figure 7. - Distribution of total- and static-pressure tubes at stations 1 and 2.

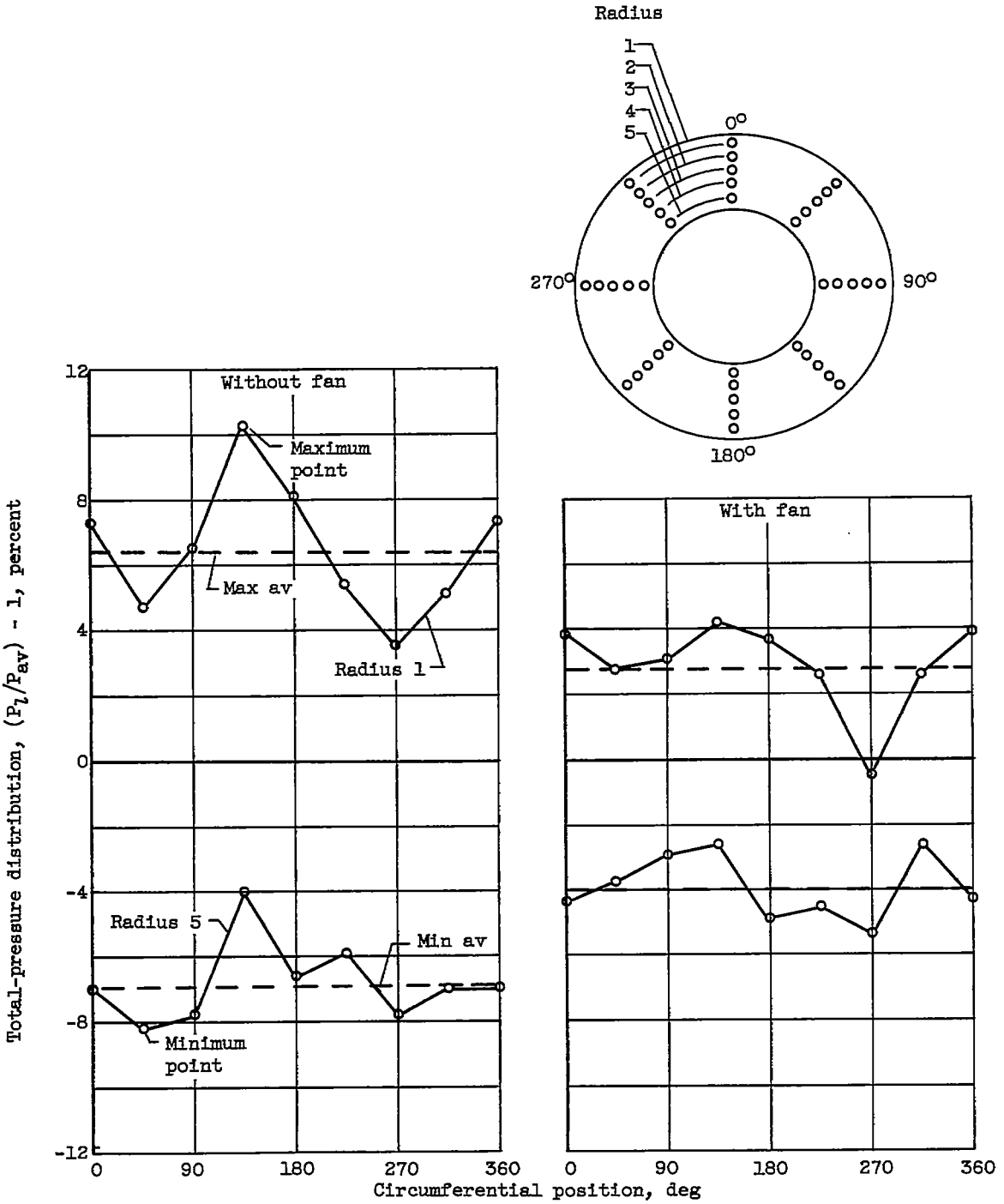


(a) Inner radial distortion; inlet annulus Mach number, 0.34; two-stage, low-solidity fan.

Figure 8. - Total-pressure profiles at station 2 indicating difference between point and average distortion.

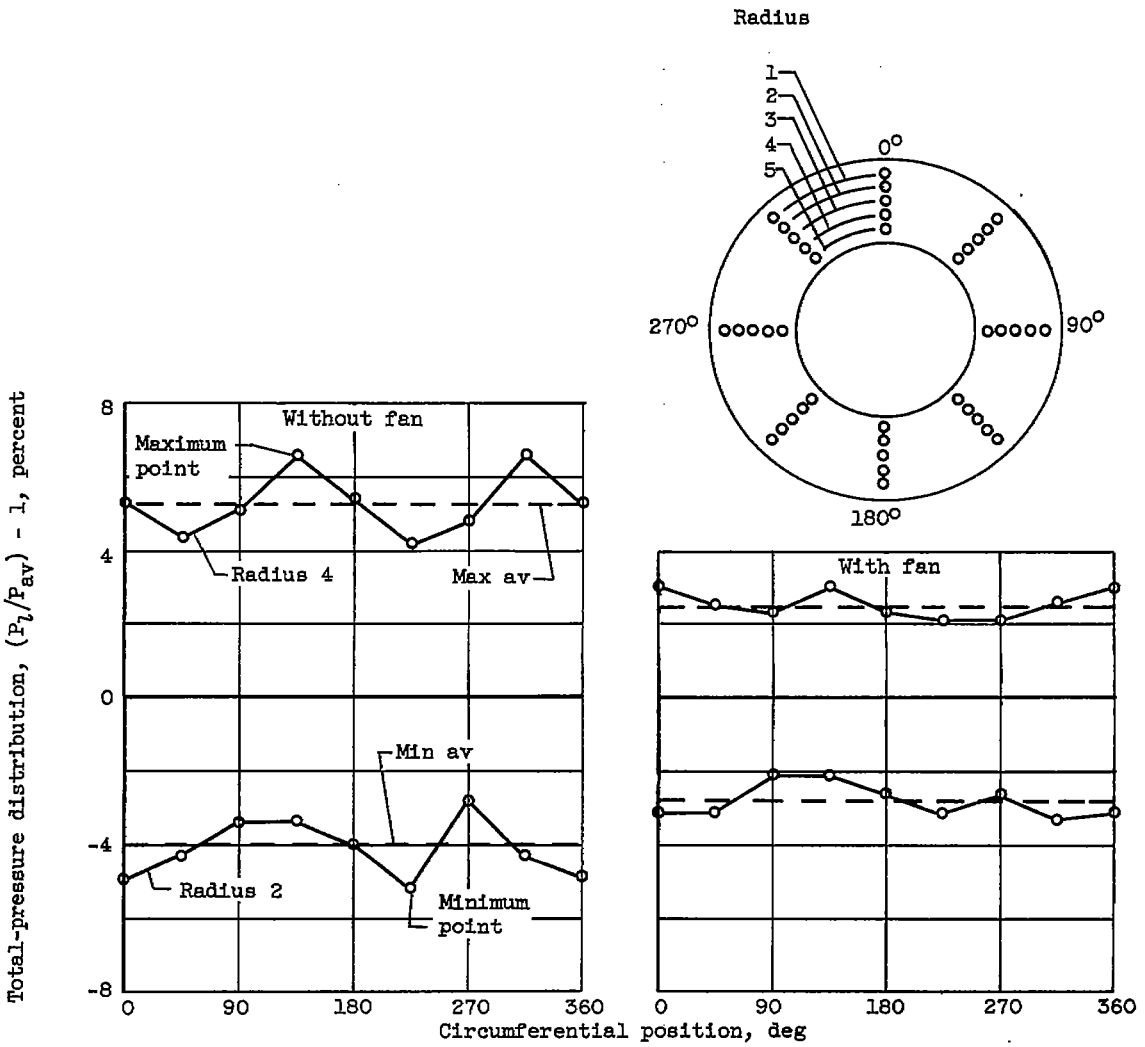


(b) Outer radial distortion; inlet annulus Mach number, 0.34; two-stage, high-solidity fan.

Figure 8. - Continued. Total-pressure profiles at station 2 indicating difference between point and average distortion.

4477

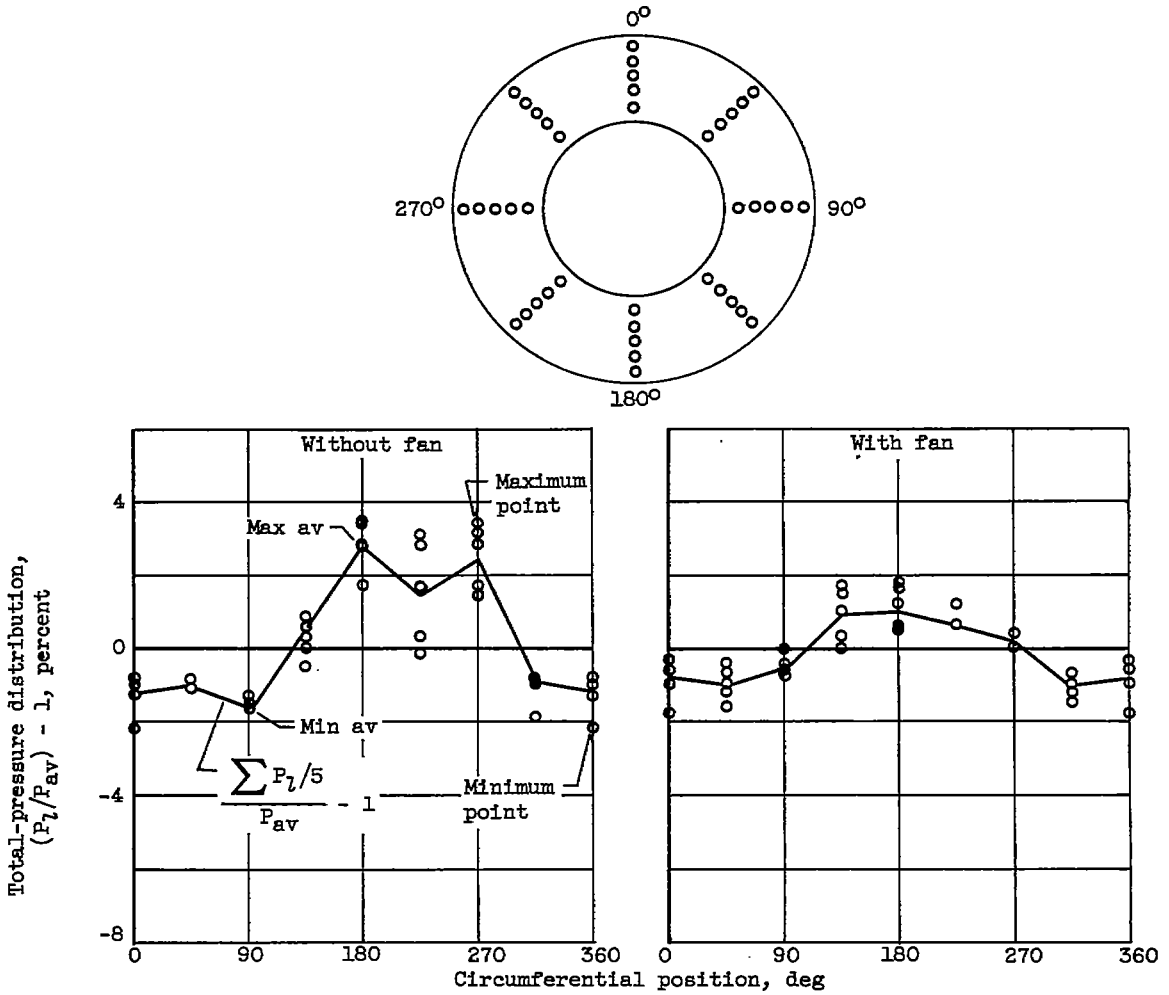


(c) Circumferential distortion; inlet annulus Mach number, 0.26; two-stage, low-solidity fan.

Figure 8. - Concluded. Total-pressure profiles at station 2 indicating difference between point and average distortion.

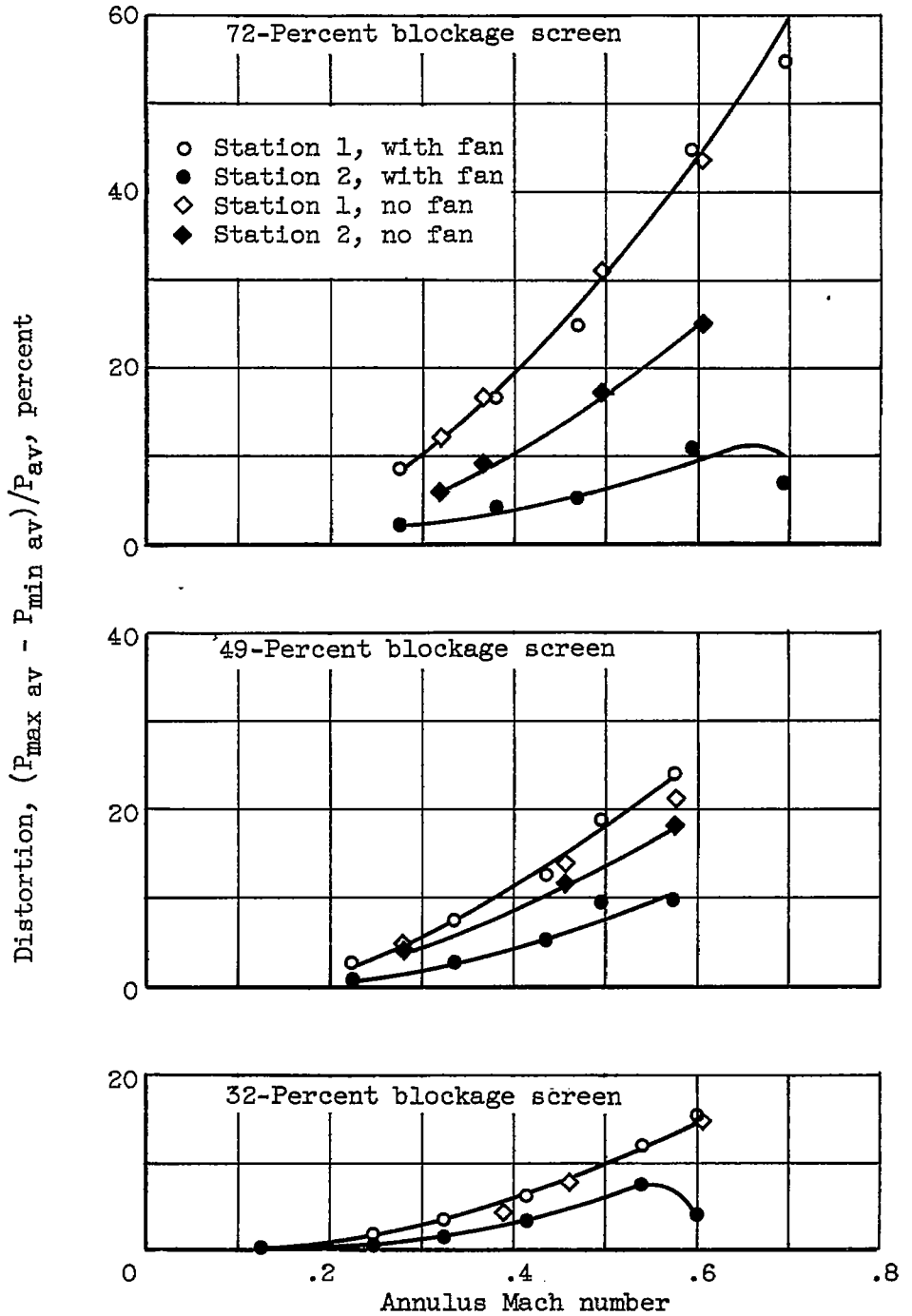


(a) Outer radial distortion.

Figure 9. - Distortion variation with annulus Mach number for various distortions. High-blade-angle fan.

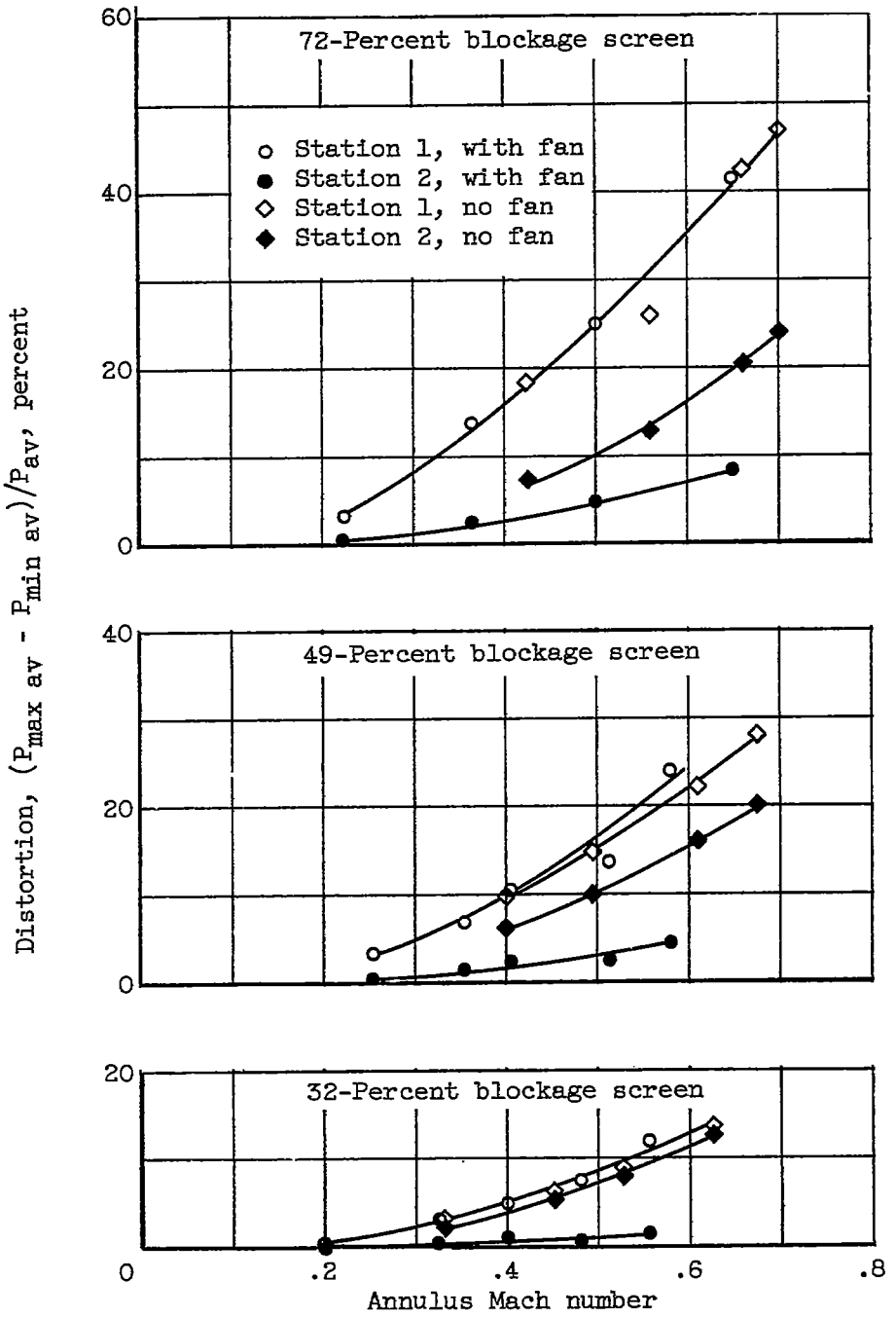


(b) Inner radial distortion.

Figure 9. - Continued. Distortion variation with annulus Mach number for various distortions. High-blade-angle fan.

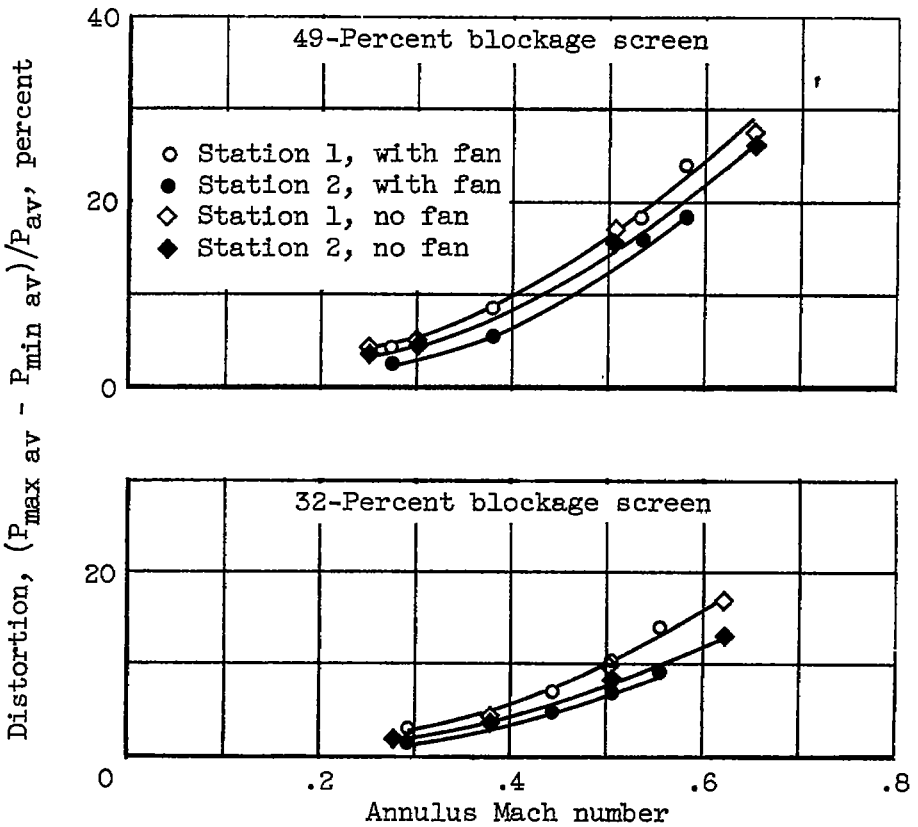


(c) Circumferential distortion.

Figure 9. - Concluded. Distortion variation with annulus Mach number for various distortions. High-blade-angle fan.

Total-pressure distribution, $(P_l/P_{av}) - 1$, percent

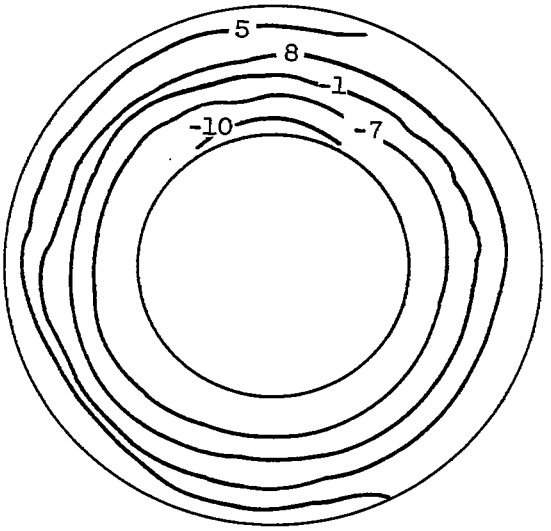


49-Percent blockage screen; annulus Mach number, 0.49

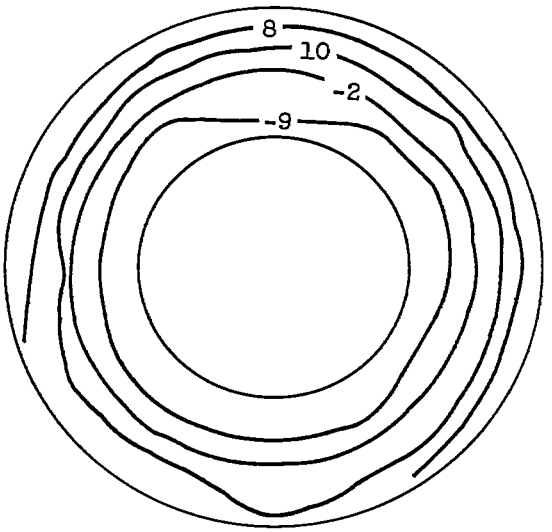


72-Percent blockage screen; annulus Mach number, 0.42

(a) Inner radial screen blockage (distortion).

Figure 10. - Typical total-pressure contours at station 2 without fan.

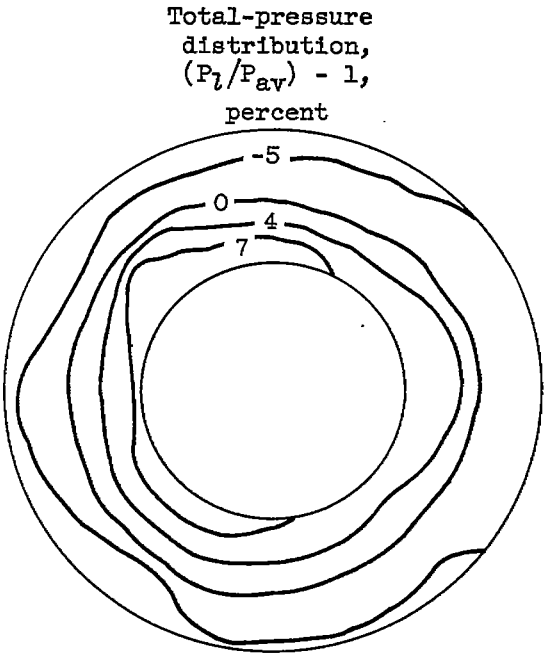


49-Percent blockage screen; annulus Mach number, 0.46

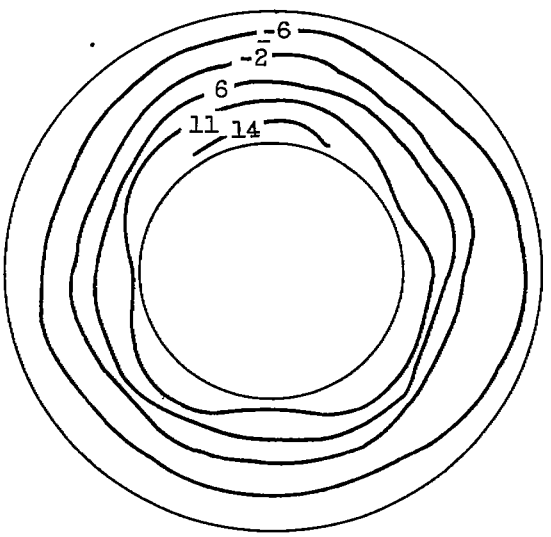


49-Percent blockage screen; annulus Mach number, 0.57

(b) Outer radial screen blockage (distortion).

Figure 10. - Continued. Typical total-pressure contours at station 2 without fan.

4477

Total-pressure distribution, $(P_l/P_{av}) - 1$, percent

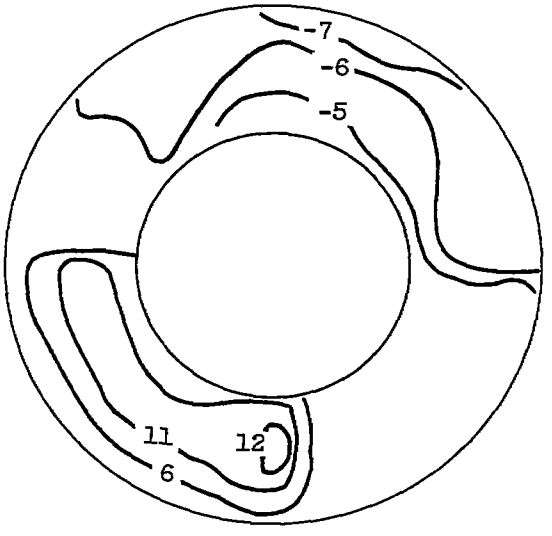


49-Percent blockage screen; annulus Mach number, 0.51

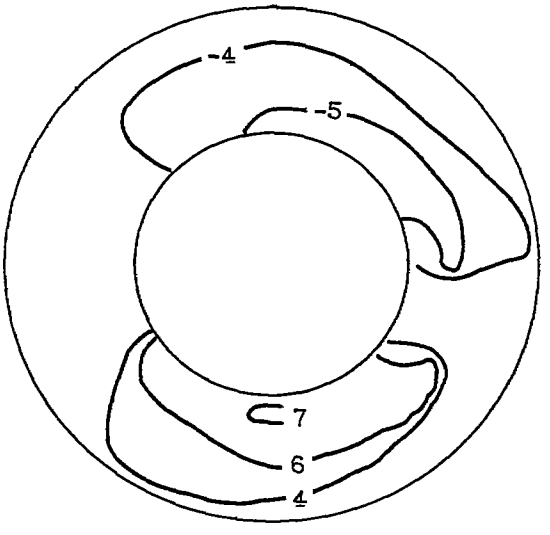


32-Percent blockage screen; annulus Mach number, 0.50

(c) Circumferential screen blockage (distortion).

Figure 10. - Concluded. Typical total-pressure contours at station 2 without fan.

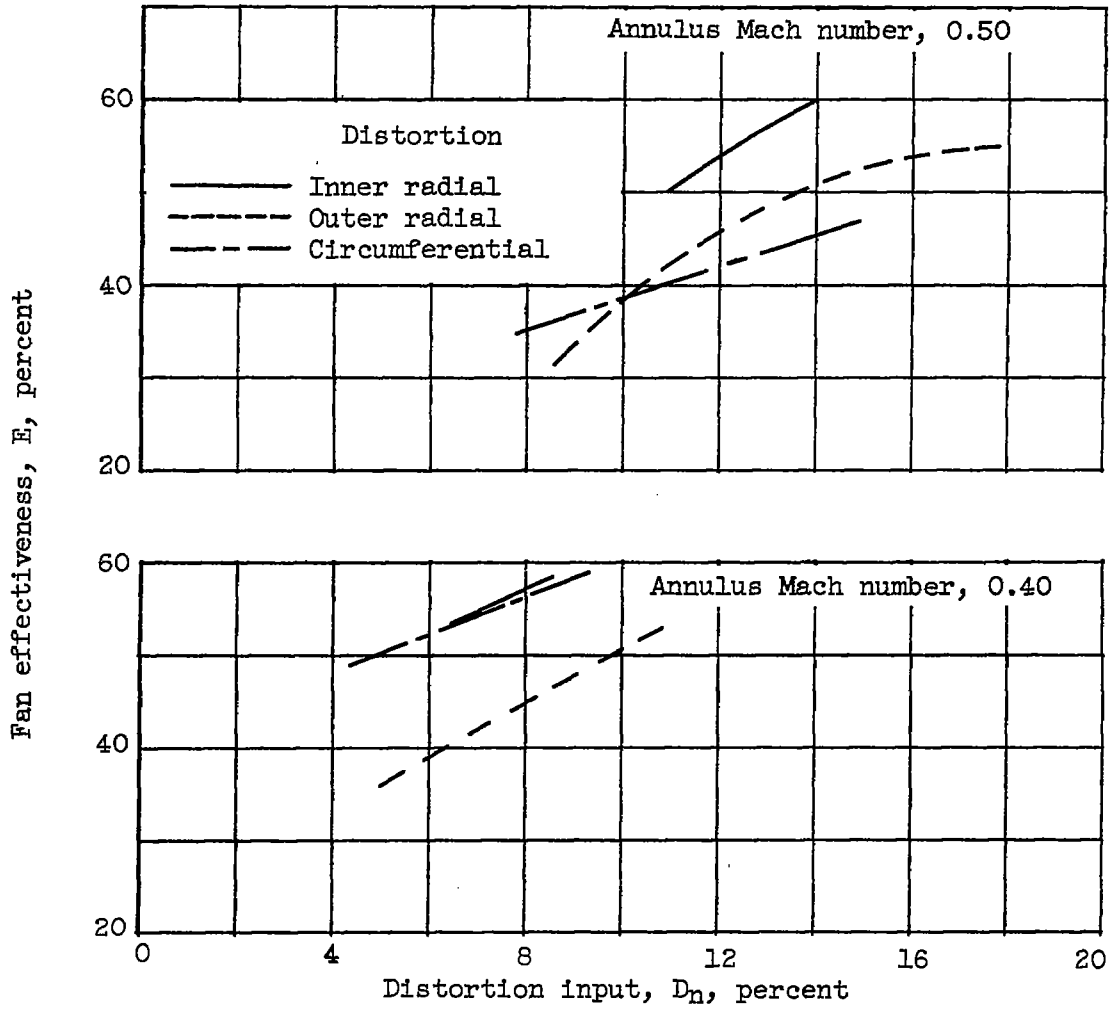


(a) Two-stage, high-solidity fan.

Figure 11. - Variation of fan distortion removal effectiveness with distortion input.

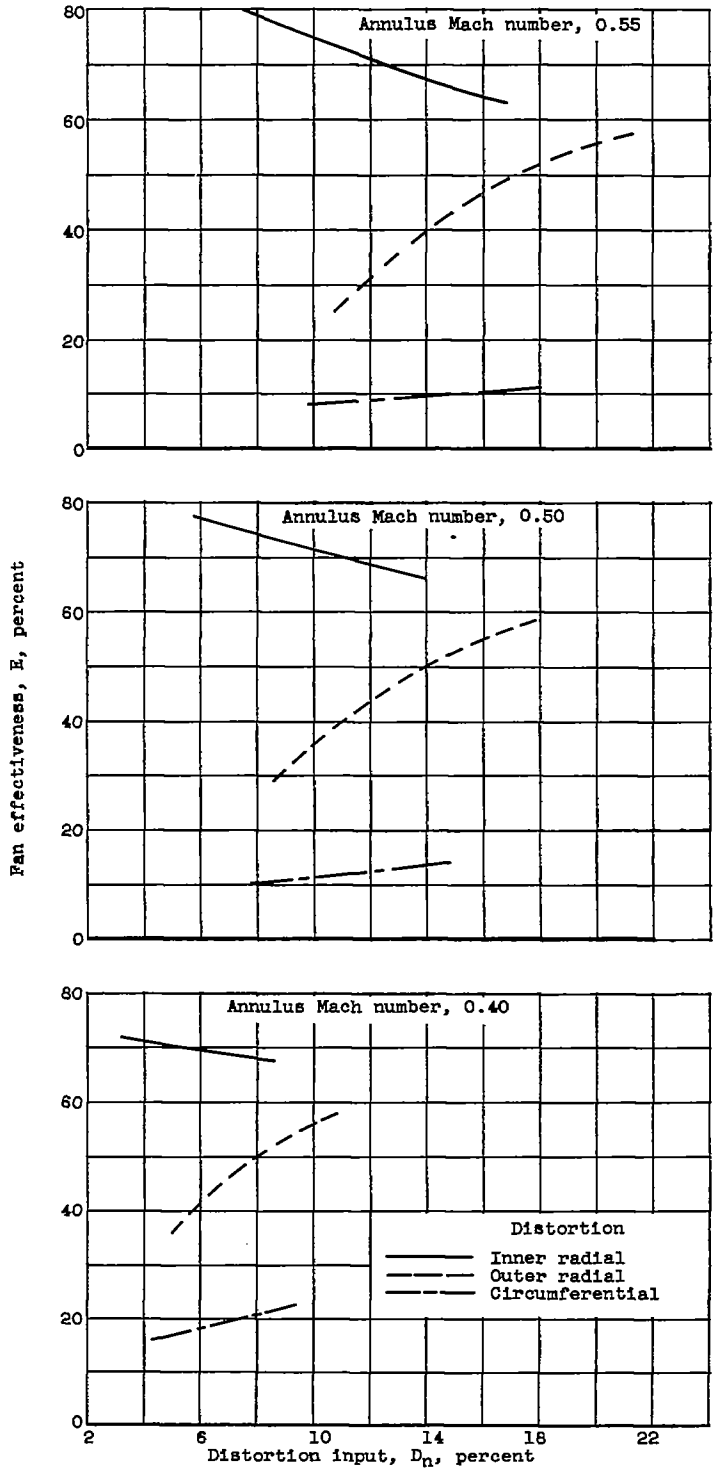


(b) Single-stage, high-blade-angle fan.

Figure 11. - Continued. Variation of fan distortion removal effectiveness with distortion input.

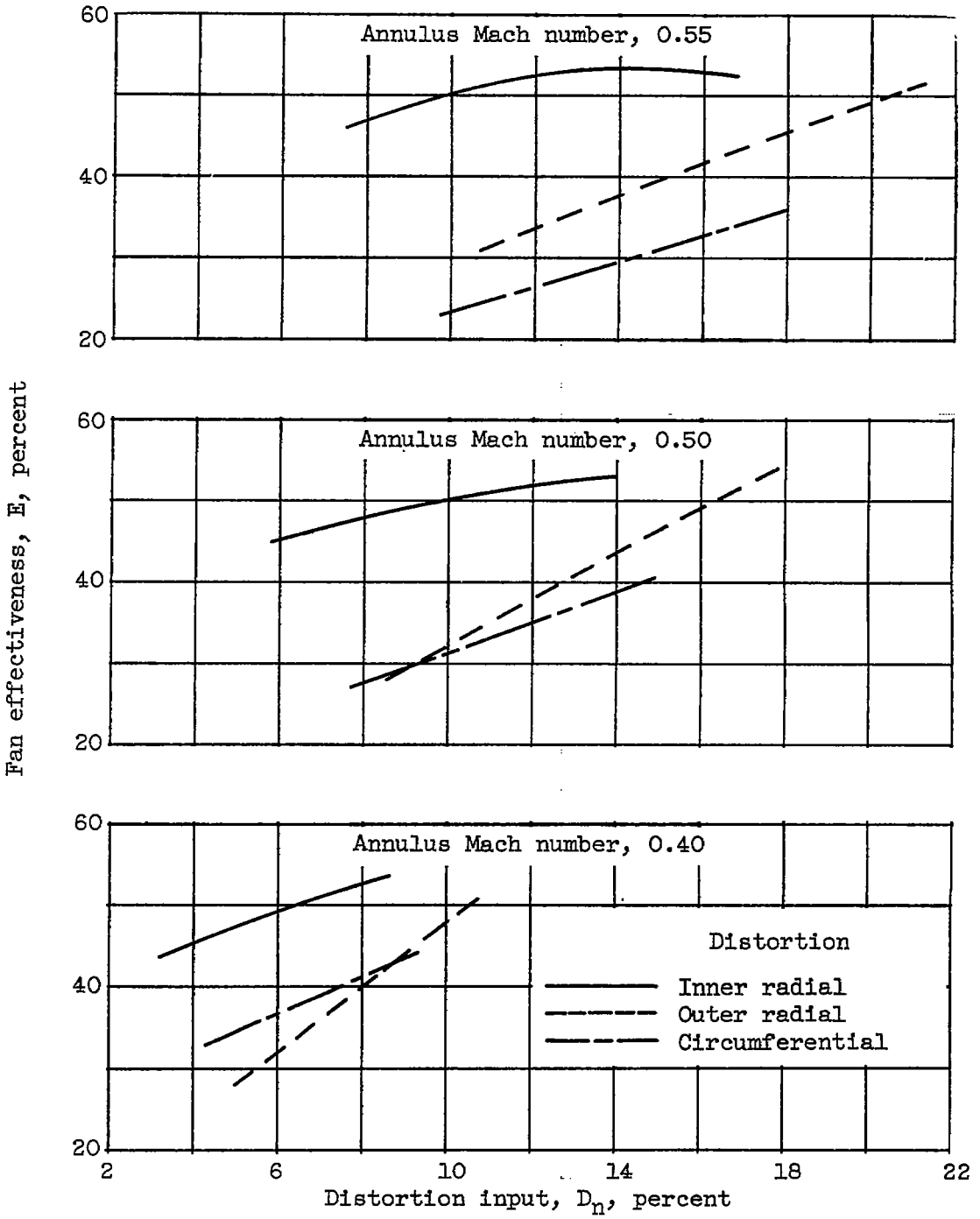


(c) Two-stage, low-solidity fan.

Figure 11. - Continued. Variation of fan distortion removal effectiveness with distortion input.

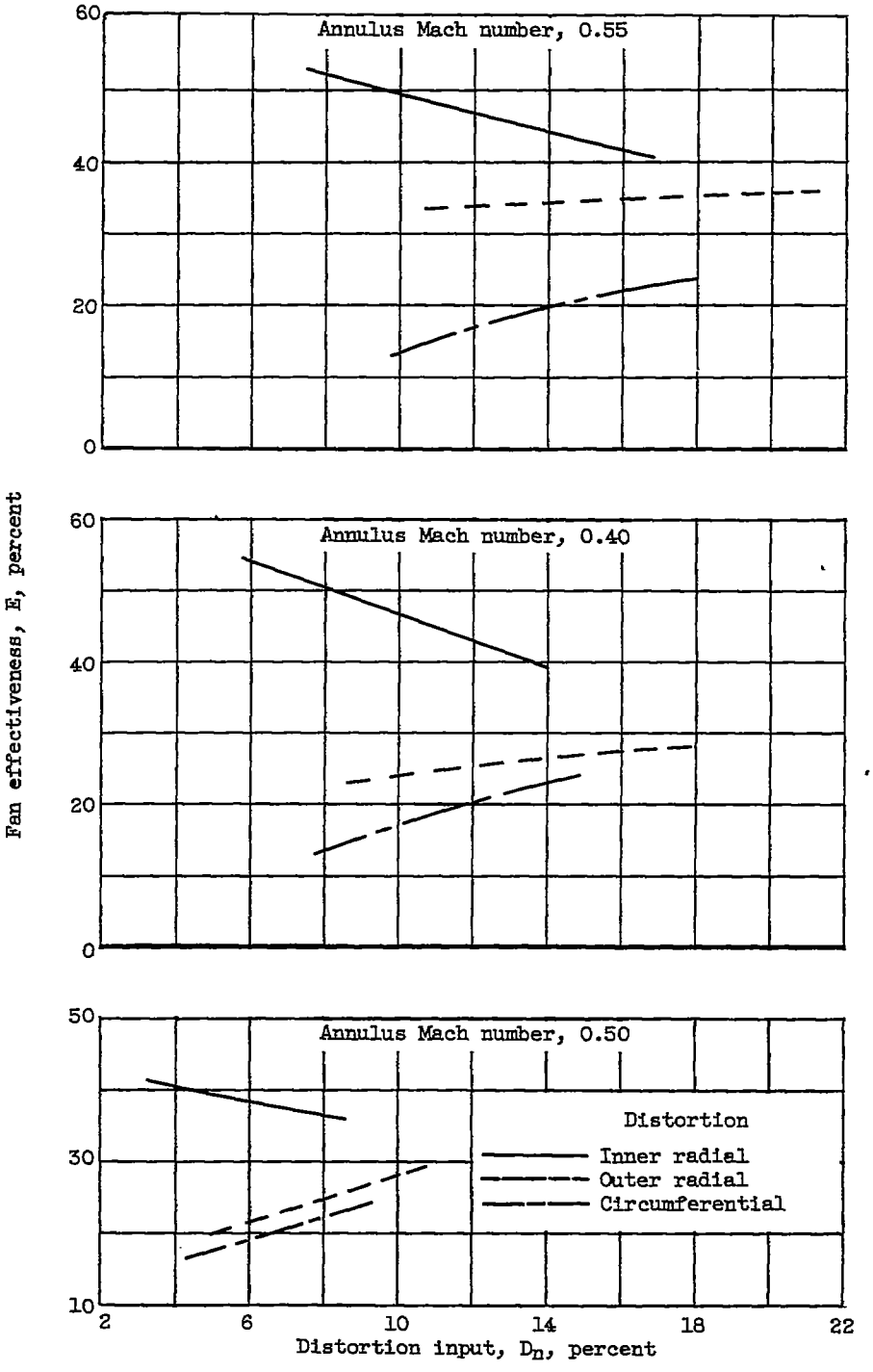


(d) Single-stage, high-solidity fan.

Figure 11. - Continued. Variation of fan distortion removal effectiveness with distortion input.

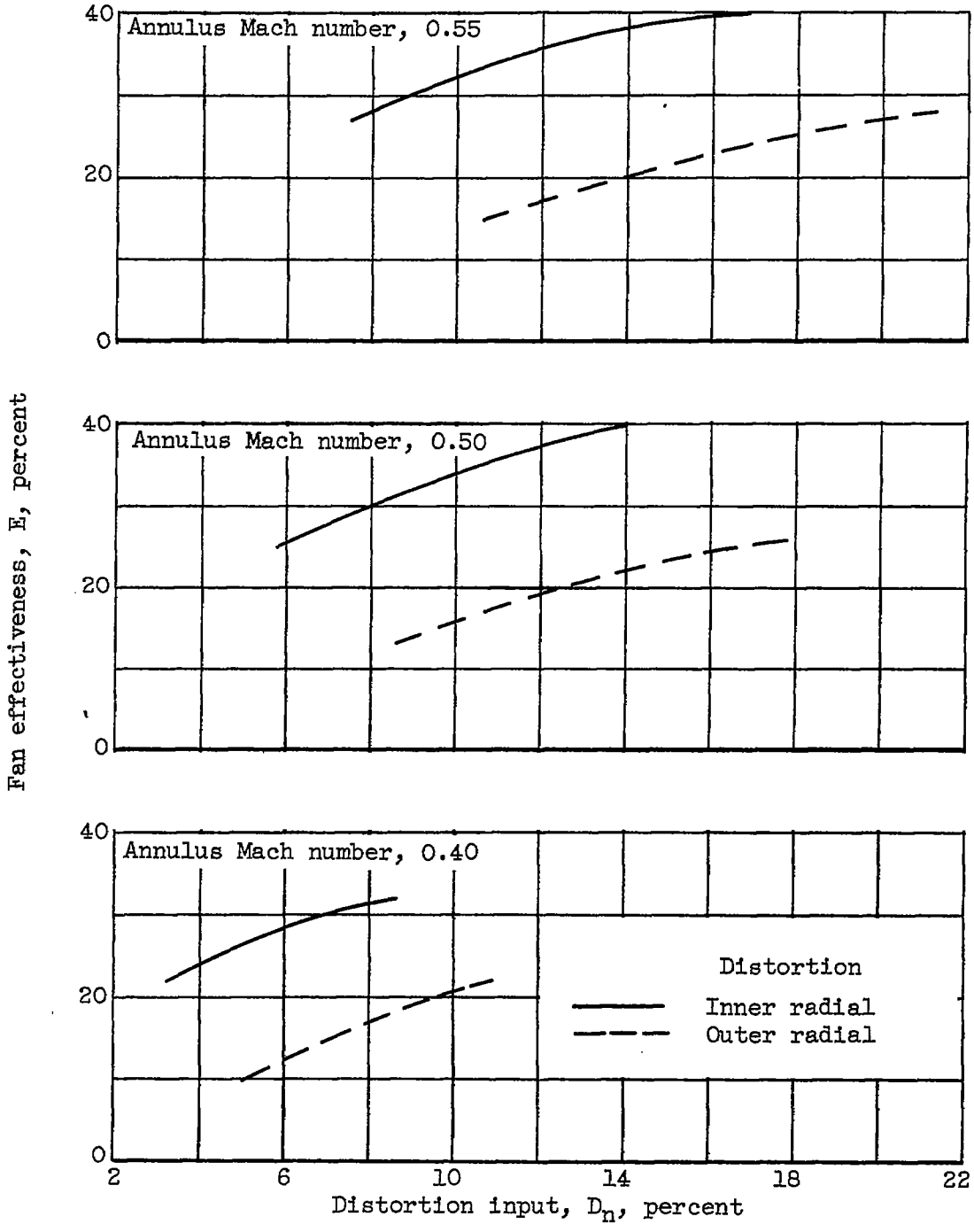


4477

(e) Single-stage, low-solidity fan.

Figure 11. - Concluded. Variation of fan distortion removal effectiveness with distortion input.

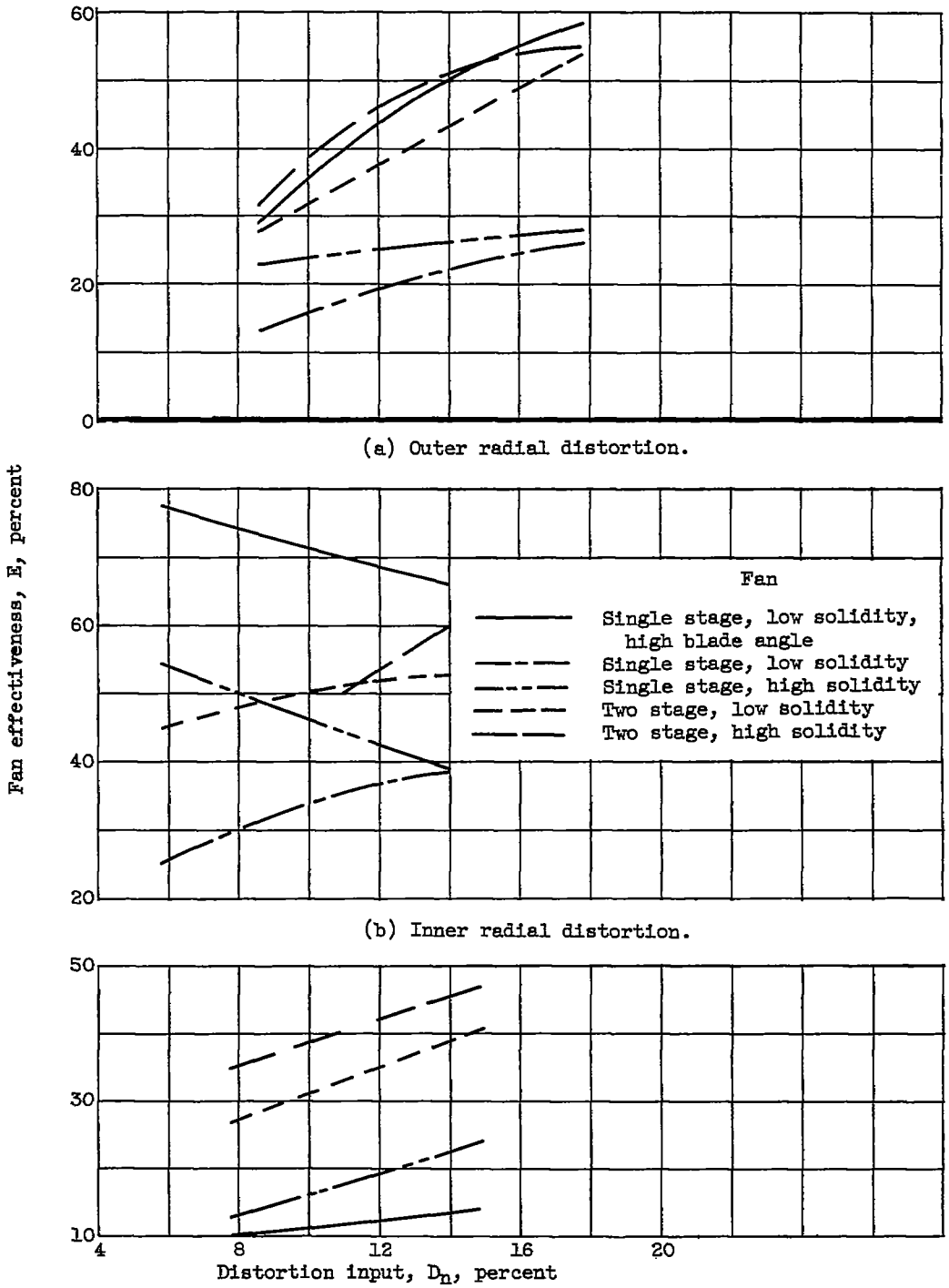


Figure 12. - Comparison of distortion removal effectiveness of various fans based on average distortion. Annulus Mach number, 0.50.

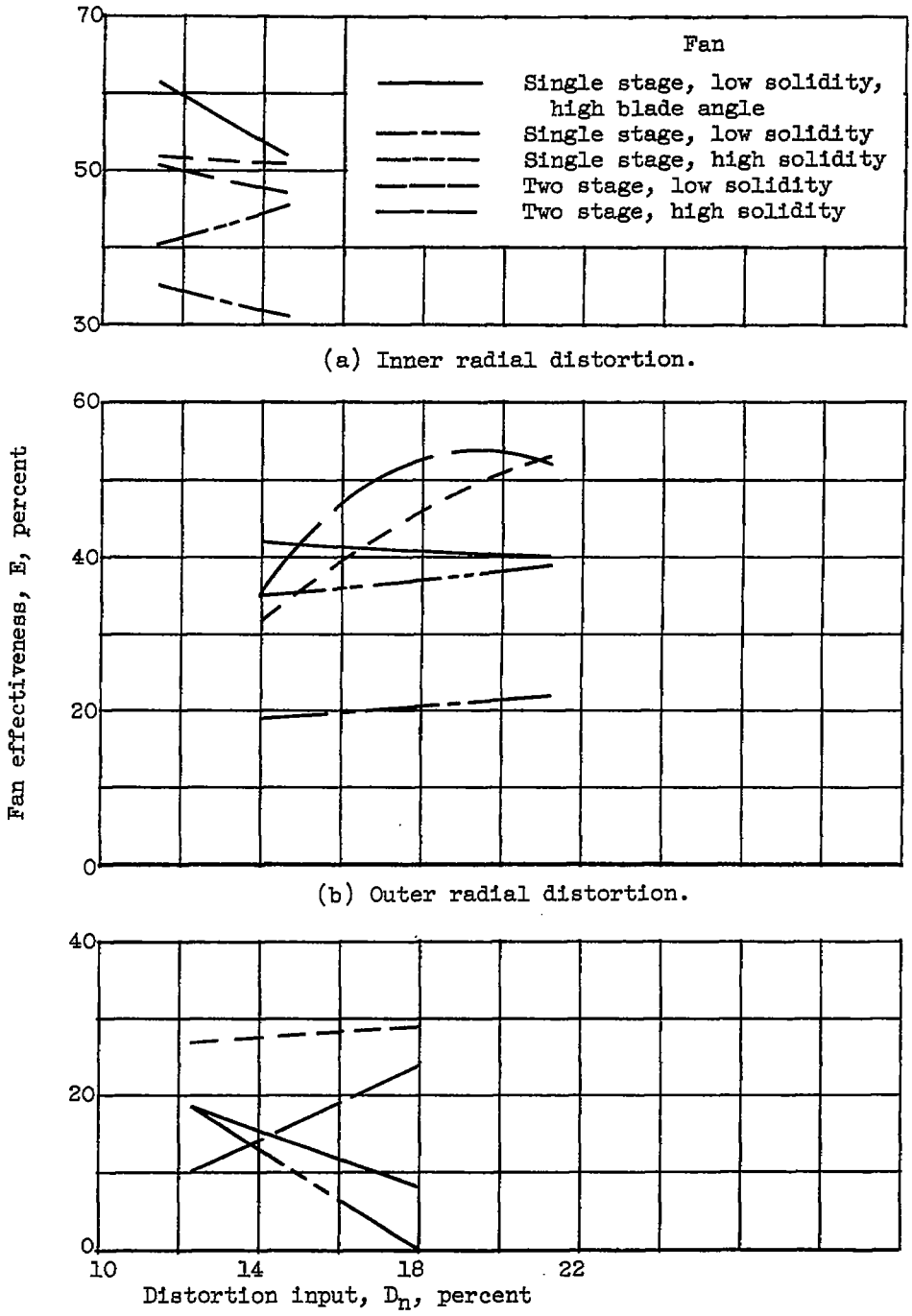


Figure 13. - Comparison of distortion removal effectiveness of various fans based on point distortion. Annulus Mach number, 0.50.

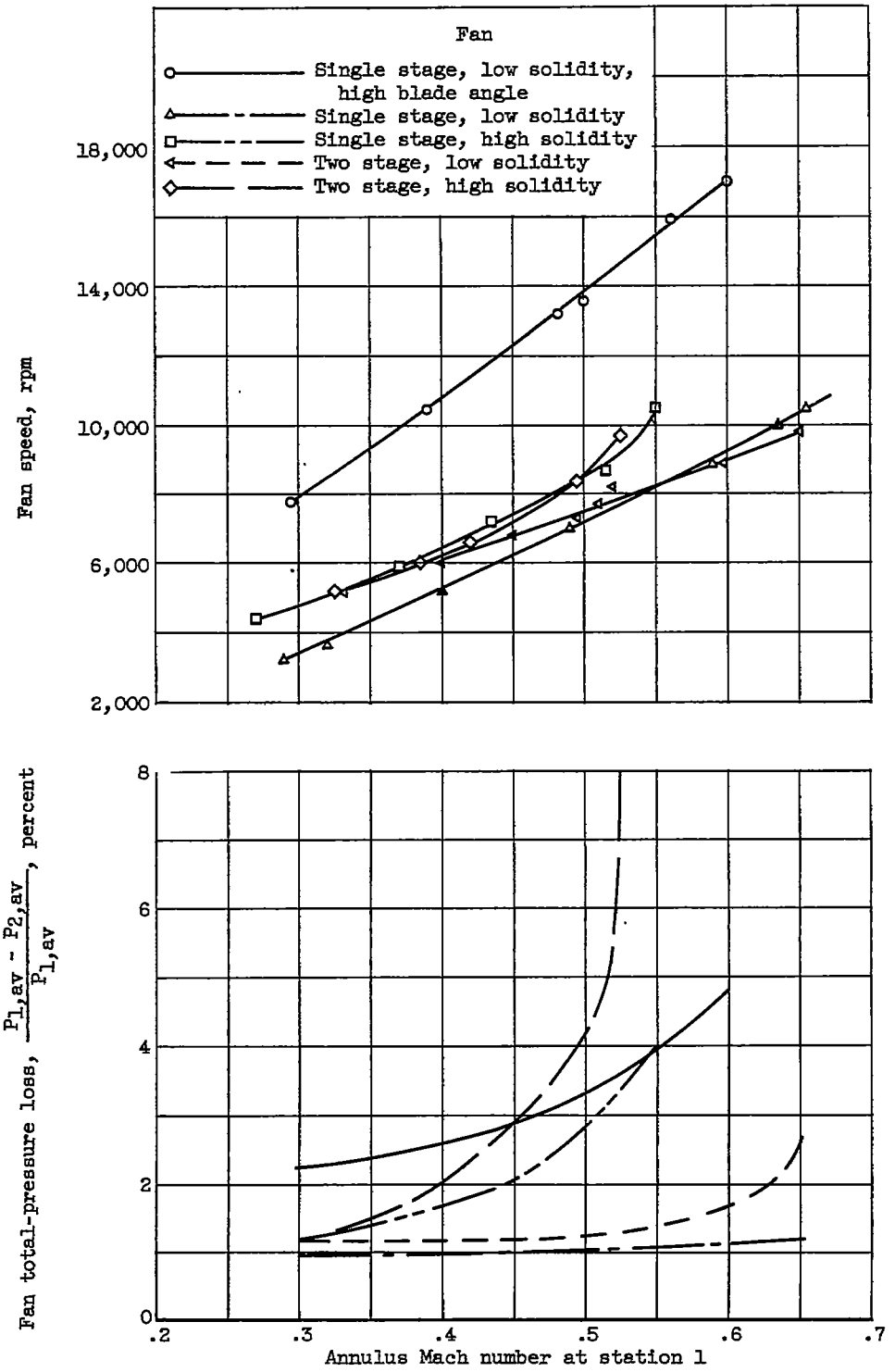


Figure 14. - Fan total-pressure loss and speed plotted against annulus Mach number for undistorted flow.